

**How to Cite:**

Malik, Z. J., & Eesa, M. J. (2022). Effect of magnesium oxide nanoparticles, hydroxyapatite and hydrogel on regeneration of transverse fracture of distal radius: Macroscopically and histologically study in rabbit model. *International Journal of Health Sciences*, 6(S2), 5094–5106. <https://doi.org/10.53730/ijhs.v6nS2.6206>

## **Effect of magnesium oxide nanoparticles, hydroxyapatite and hydrogel on regeneration of transverse fracture of distal radius: Macroscopically and histologically study in rabbit model**

**Zainab J. Malik**

Department of Surgery and reproductive science, Veterinary Medicine College, Al-Qasim Green University, Iraq

**M J. Eesa**

Department of Surgical and reproductive science, Veterinary Medicine College, Baghdad University, Iraq

**Abstract**---Study's purpose of this study is to conduct synthesis and evaluate the effect of hydroxyapatite (HA) with hydrogel locally magnesium oxide nanoparticles (MgONPS) locally or intraperitoneally (IP) on the healing of the distal third radial fracture. Concentrations of MgONPs 200µg/ml, dissolved in 1 cc distilled water and the solution stirred by a stirrer for 10 min. HA 0.5 mg in 1ml hydrogel and the solution stirring at the vortex for 15 min. These materials were evaluated in vitro to ensure their suitability with the tissues. Seventy-five healthy adult male rabbits, aged about 1.5- 2 years old with average weighting 1.7- 2.3 Kg. B.W were used. Rabbits were divided into three groups randomly (n=25), group A (HA mixed hydrogel applied locally), group B (HA mixed with hydrogel and MgONPs applied locally) and group C (HA mixed hydrogel applied locally and MgONPs IP). Animals were anesthetized by i.m 40 mg/ kg B.W ketamine hydrochloride and 5mg/ kg B.W xylazine. A 5cm incision had made cranio-medially in the skin of the forelimb (right forelimb) and exposure radius and ulna. The macroscopic evaluation revealed that all groups at 2nd week showed bone reaction in different degrees. At the 4<sup>th</sup>-week post-operation, all groups showed partially connected fracture ends. At the 8<sup>th</sup>-week postoperative, the bone fractured the normal shape, especially groups B and C. Histopathological examination revealed that group A at 2<sup>nd</sup> weeks post-operation showed trabecular bone formation. At 4<sup>th</sup>-weeks post-operation of the same group showed active osteoblast remnant of vascular congestion,

at 8<sup>th</sup> weeks showed endochondral ossification with osteoid deposition and new hyaline cartilage formation. In group B at 2<sup>nd</sup> week post-operative showed hyaline cartilage in compact bone with active osteoblast lining, at 4<sup>th</sup>-week lamellar bone with calcified osteoid tissues, at 8<sup>th</sup> week revealed compact bone with fewer hyaline cartilage. In group C at 2<sup>nd</sup> of endochondral ossification, at 4<sup>th</sup> week showed compact bone, at an 8<sup>th</sup>-week good area of compact bone.

**Keywords**---transverse fracture, MgO NPs, HA, hydrogel, rabbit.

## Introduction

The long bones fractures healing may be impaired and eventually end in delayed union and non-union, commonly long bone like radius, had problems lead to use many materials to bypass these problems (1 and 2). Hydroxyapatite (HA) is an inorganic component of bone considered and for its bioactivity, biocompatibility, biointegrating, and osteoconductive property used in engineering bone tissue (3 and 4). Calcium phosphates (CaP) are biodegradable and biocompatible materials for bone regeneration to support tissue regeneration (5). Magnesium (Mg) is the fourth common metal element that plays an important role in mineral metabolism and osteogenesis (6 and 7). It stimulates bone formation by accelerating mineralization and regulating cell adhesion and differentiation (8, 9 and 10). Magnesium doped hydroxyapatite (Mg-HA) controls the initial degradation rate, accelerates new bone formation on the implant material, and guides bone regeneration (11). Nanomaterials were used in biomedical applications because they have good physicochemical, biocompatibility properties and ease of functionalization (12, 13 and 14). MgONPs have antibiotic activity and accelerate osteogenic differentiation, which attracted considerable attention in tissue engineering (15 and 16). When added MgONPs to hydroxyapatite found that MgONPs and hydroxyapatite influence preosteoblast cell behaviours such as adhesion, proliferation, and differentiation (17). Different bioactive metal and metal oxide nanoparticles were inlays by hydrogels, such as Mg (18), they eventually can be absorbed or decomposed by new bone tissue formation without rejection (19 and 20).

## Materials and Methods

### Experimental Animals

Seventy-five adult male rabbits average aged 1.7 years with average weighting 1.7- 2 Kg. B.W were used. They were housed in special cages in the College of Veterinary Medicine after obtaining official approval from the ethical committee of the Veterinary Medicine College, the University of Baghdad, after doing let study MgONPs dose was selected at 200µg/ml, dissolved in 1 ml distilled water and stirring for 10 min., recommended this dose by (Wetteland *et al.*; 2017). HA 0.5 mg in 1ml gel and stirring the solution for 15 min at the vortex (21).

## Experimental Design

Seventy-five experimental animals were divided into three equal groups:

Group A: In which animals of this group were subjected to complete transverse fracture at the distal third of the radius and after induced fracture, a mixture of HA with gel was applied locally at the fracture

Group B: Same as in group A, but HA/gel and MgONPs mixture was applied locally.

Group C: Same as in group A, but after induced fracture, a mixture HA with gel locally at fracture site and MgONPs "suspension was injected IP.

## Biosynthesis Magnesium Oxide Nanoparticles preparation

To prepare the aloe vera extract must be cut the leaf and washed with tap water. 15 gr of aloe vera was mixed with 150 mL of distilled water and stirred at 80°C for 60 min and cooled this mixture at room temperature and before added aloe vera extract with Manganese (II) sulphate as the precursor filtered it, then these products were exposed in to ultrasonic at 30 min. and later at shaker for 24hr, finally at centrifuge for 30min., the precipitate was dried in an incubator at 80°C (21) (Fig. 1). At the end collected, the MgONPs powder.

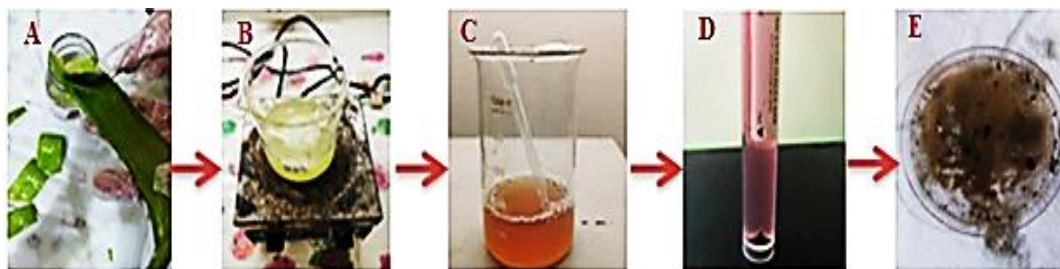


Figure 1: Steps of biosynthesis of MgONPs using aloe vera extract (A) Aloe vera leaf after cleaning and cutting. (B) Gel of leaf with 150 mL of distilled water and Stirred at 80°C for 60 min. (C) The mixture of aloe vera plant extract and Manganese (II) sulphate. (D). The precipitate was obtained after centrifuging for 30min. (E) dry particles of MgONPs.

## Characterization of Magnesium oxide nanoparticles

Atomic Force Microscopy (AFM) analysis: The surface morphology and particle size of Magnesium Oxide Nanoparticles were carried out using Atomic force Microscope (on AA 3000 Scanning probe microscope Angstrom Advanced) (23).

UV -Vis analysis: The reduction of pure Mg<sup>+</sup> was monitored by measuring the UV-Vis spectrum of the reaction medium after 30 min. It is procured from Shimadzu. A small aliquot of the sample was taken for UV-Vis spectrum analysis (200-800 nm) (24).

## Characterization of Hydroxyapatite

The characterized by different analytical techniques XRF measurements performed in the Science and technology ministry, Iraq

X-Ray Fluorescence (XRF): It is a non-destructive technique that allows, not only to screen the elements present in a sample (HA), (qualitative analysis), as well as to establish the proportion (concentration) at which each element is present in the sample. In XRF, a source of high energy radiation (gamma or X rays) excites the atoms present in the substance of interest. When an atom in the ground state is exposed to an external power source (eg: an Xray), it absorbs energy, promoting the electrons to higher energy levels. In these states, the atom is at an unstable situation, called "excited state" (25).

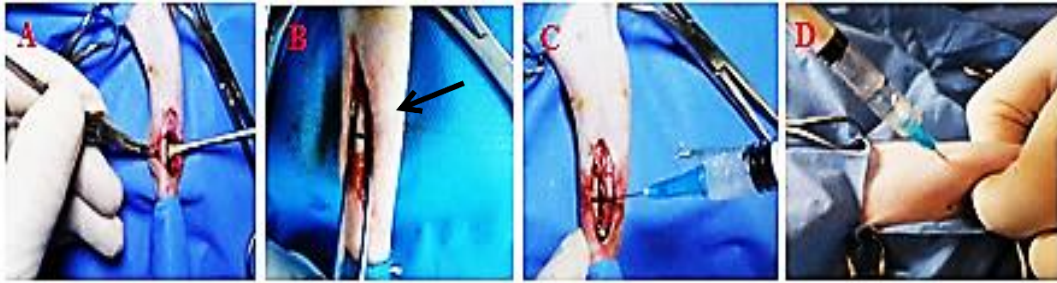
### **Hydrogel preparation**

Carbopol 0.125 g was dispersed in distilled water 6.25 w/w 2% by stirring at 800 rpm for 60 min and adjusted with NaOH 10% dropwise was added and adjusted with methanol drop wise was added to prevent the contamination . That mixed until a transparent gel formed and the pH was neutral approximately. The gels must be reserved at 4°C 12 h before using until air bubbles removed,(26). This working at the pharmacological department of veterinary medicine college in Baghdad university.

### **Characterization of hydrogel gel**

The Irritation test Injected 1ml from each of carbopol, Al-cohol, HA, MgONPs, HA+MgONPs, carbopol+ Al-cohol +MgONPs, carbopol+ Al-cohol+ HA and carbopol+ Al-cohol+ HA+MgONPs. After 1h. and B after 24h. to observed the irritant of the gel element before and after mixed with HA and MgONPs. All of characterized by different analytical techniques measurements were performed in the pharmacological department of vetrenary medicine college, university of Baghdad.

Surgical operation The animal was prepared from midshift of humerous to mide-shift of metacarpus bones aseptically for operation after general anasethetic A 5cm incision was made cranio-medially in the skin of the forelimb and the right radius was exposed by dissecting between flexor carpi radialis and extensor carpi radialislongus (Figure 2.A). Osteotomies was performed to create transverse fracture of the distal radius (Figure 2.B). In group A and B applied a mixture of HA and gel, HA and gel with MgONPs, a mixture of HA and gel locally at fracture site and give the MgONPs IP respectively (Figure 2.C and D). The subcutaneous tissue and muscle was closed in separate layers using polyglactin 910 (3.0) sutures material by simple continuous pattern and closed the skin by subcuticular suture pattern, finally fixation the fracture externally with modified aluminum plate (27).



Figure, 2: Show (A) exposed right radius. (B) Osteotomies were performed to create a fracture. (C) show injected materials at the fracture site in groups A, B and C (D) injected of MgONPs solution intraperitoneally in group C.

**Macroscopic Evaluation:** In all experimental animals, the radial bone fractured was dissected from the surrounding tissue and macroscopic examination at 2, 4 and 8 weeks post-operatively to evaluate the amount of callus fracture and degree of healing. **Histopathological Evaluations:** Bone specimens were obtained at 2, 4, and 8 weeks post-operatively from all animals groups. The specimens were fixed in 10% neutral buffer formalin for 72 hr after that decalcification using a mixture of formic acid solution and sodium citrate for two weeks (or until complete decalcification of bone). After several chemical processes, the samples were sectioned into 5 $\mu$ m with a microtome (Leica SP 1600; Leica Microsystems, Germany), and finally stained with Hematoxylin and Eosin and view under a light microscope (AX80T; Olympus, Tokyo, Japan) to evaluate the healing degree of fracture site (28).

## Results

### Laboratory Evaluation of Magnesium Oxide Nanoparticle

**Atomic Force Microscopy (AFM):** This technique refers to digital images that allow measurements of surface features, such as average roughness (Ra), root means square roughness (Rq) and the analysis of images from different perspectives, including 3D simulation. Fig. 3, The three dimensional AFM images and granularity distribution of the MgO NPs very important to note that the mean values were obtained and showed a statistical variance (23). The average size for the MgO NPs in the present study was 65.04 nm,

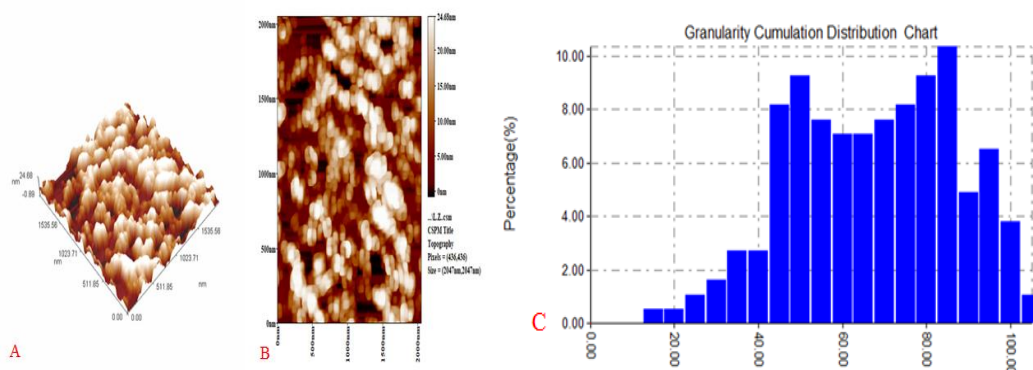
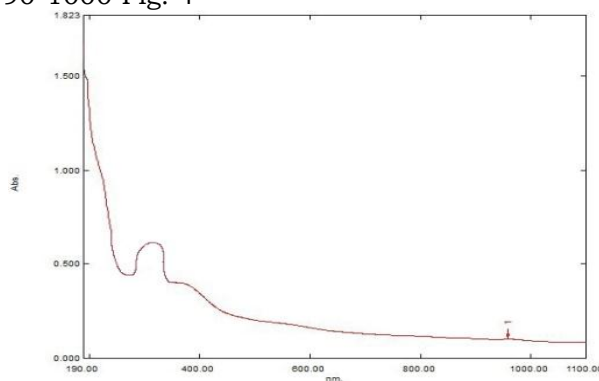


Figure 3: AFM images (A) three dimensions, (B) two dimensions, and (C) histogram of the distribution of grain size.

The optical absorption analysis (UV. Visible) UV-VIS is the optic absorption spectrum. The absorption spectra of the MgO were recorded within the wavelengths of 190-1000 Fig. 4



Figure, 4: UV-Vis. spectrum of the MgONPs synthesis by Alovera extract

### Laboratory Evaluation of Hydroxyapatite (HA)

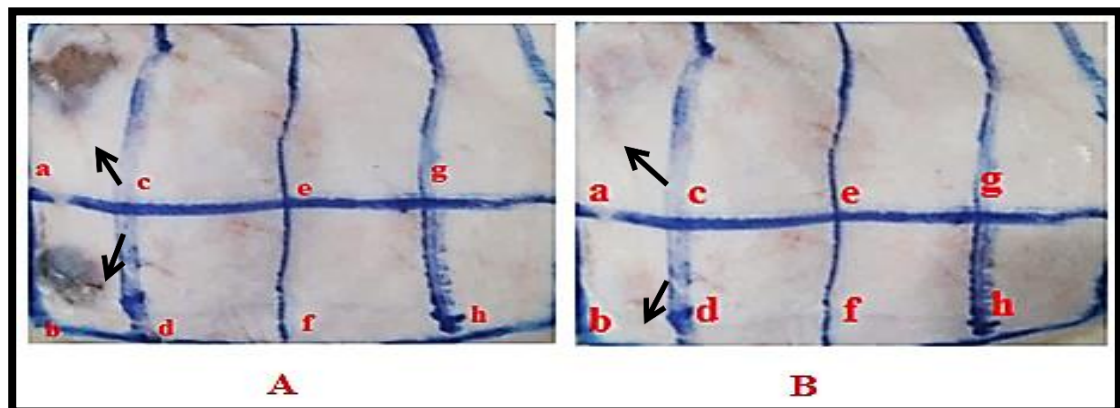
X-Ray Fluorescence (XRF): This analyzes the elements and compounds of (HA) composed of and their relative amount. Table 1. The HA sample was analysed using multifunctional energy dispersive X-ray fluorescence spectrometer as medium samples when prepared as pellets. elements concentrations were measured by this technique: Ca, Pb, P, Cu, ...et ct. ;

Table 1: show the concentration of essential elements that compounds the HA

Z	Symbol	Element	Concentration	Abs. Error	Z	Symbol	Element	Concentration	Abs. Error
11	Na	Sodium	< 0.49 %	(0.0) %	11	Na2O		< 0.66 %	(0.0) %
12	Mg	Magnesium	< 0.076 %	(0.0) %	12	MgO		< 0.13 %	(0.0) %
13	Al	Aluminum	< 0.020 %	(0.0) %	13	Al2O3		< 0.038 %	(0.0) %
14	Si	Silicon	< 0.011 %	(0.0) %	14	SiO2		< 0.023 %	(0.0) %
15	P	Phosphorus	5.125 %	0.007 %	15	P2O5		11.74 %	0.02 %
16	S	Sulfur	< 0.00083 %	(0.0) %	16	S2O3		< 0.0021 %	(0.0) %
17	Cl	Chlorine	< 0.00029 %	(0.0) %	17	Cl	Chlorine	< 0.0029 %	(0.0) %
19	K	Potassium	0.0376 %	0.0022 %	19	K2O		0.2453 %	0.0027 %
20	Ca	Calcium	32.11 %	0.04 %	20	CaO		44.83 %	0.06 %
22	Ti	Titanium	< 0.00050 %	(0.0) %	22	TiO2		< 0.0083 %	(0.0) %
23	V	Vanadium	< 0.00051 %	(0.0) %	23	VO2		< 0.0091 %	(0.0) %
24	Cr	Chromium	< 0.0021 %	(0.0) %	24	CrO3		< 0.0030 %	(0.0) %
25	Mn	Manganese	0.0040 %	0.0010 %	25	MnO		0.0062 %	0.0013 %
26	Fe	Iron	0.0365 %	0.0013 %	26	Fe2O3		0.0026 %	0.00048 %
27	Co	Cobalt	0.00178 %	0.00038 %	27	CoO		< 0.0021 %	(0.00026) %
28	Ni	Nickel	< 0.00040 %	(0.00023) %	28	NO		0.00171 %	0.00031 %
29	Cu	Copper	0.00136 %	0.00024 %	29	CuO		0.00098 %	0.00019 %
30	Zn	Zinc	0.00069 %	0.00015 %	30	ZnO		< 0.0021 %	(0.0) %
31	Ga	Gallium	< 0.00021 %	(0.0) %	31	Ga	Gallium	< 0.00019 %	(0.0) %
32	Ge	Germanium	< 0.00019 %	(0.0) %	32	Ge	Germanium	< 0.00022 %	(0.0) %
33	As	Arsenic	< 0.00017 %	(0.0) %	33	As2O3		0.00006 %	0.00006 %
34	Se	Selenium	0.00006 %	0.00006 %	34	Se	Selenium	< 0.00011 %	(0.0) %
35	Br	Bromine	< 0.00011 %	(0.0) %	35	Br	Bromine	0.00016 %	0.00007 %
37	Rb	Rubidium	0.00015 %	0.00007 %	37	Rb2O		0.01934 %	0.00020 %
38	Sr	Strontium	0.1635 %	0.00017 %	38	SrO		0.00085 %	0.00006 %
39	Y	Yttrium	0.00085 %	0.00008 %	39	Y	Yttrium	< 0.0031 %	(0.0) %
42	Mo	Molybdenum	< 0.0021 %	(0.0) %	42	Mo	Molybdenum	< 0.0063 %	(0.0) %
47	Ag	Silver	< 0.00003 %	(0.0) %	47	Ag	Silver	< 0.00057 %	(0.0) %
48	Cd	Cadmium	< 0.00057 %	(0.0) %	48	Cd	Cadmium	< 0.0012 %	(0.0) %
50	Sn	Tin	< 0.00051 %	(0.0) %	50	SnO2		< 0.00095 %	(0.0) %
51	Sb	Antimony	< 0.00045 %	(0.0) %	51	Sb	Antimony	< 0.0012 %	(0.0) %
52	Te	Tellurium	< 0.0012 %	(0.0) %	52	Te	Tellurium	< 0.0024 %	(0.0) %
53	I	Iodine	< 0.0024 %	(0.0) %	53	I	Iodine	< 0.0045 %	(0.0) %
56	Ba	Barium	< 0.0040 %	(0.0) %	56	BaO	Barium	< 0.00090 %	(0.0) %
74	W	Tungsten	< 0.00071 %	(0.0) %	74	WO3		< 0.00031 %	(0.00018) %
80	Hg	Mercury	< 0.00031 %	(0.00018) %	80	Hg	Mercury	< 0.00030 %	(0.0) %
81	Tl	Thallium	< 0.00030 %	(0.0) %	81	Tl	Thallium	0.00048 %	0.00020 %
82	Pb	Lead	0.00045 %	0.00018 %	82	PbO		< 0.00025 %	(0.0) %
83	Bi	Bismuth	< 0.00025 %	(0.0) %	83	Bi	Bismuth	0.00035 %	0.00013 %
90	Th	Thorium	0.00035 %	0.00013 %	90	Th	Thorium	< 0.00026 %	(0.0) %
92	U	Uranium	< 0.00026 %	(0.0) %	92	U	Uranium	< 0.00026 %	(0.0) %

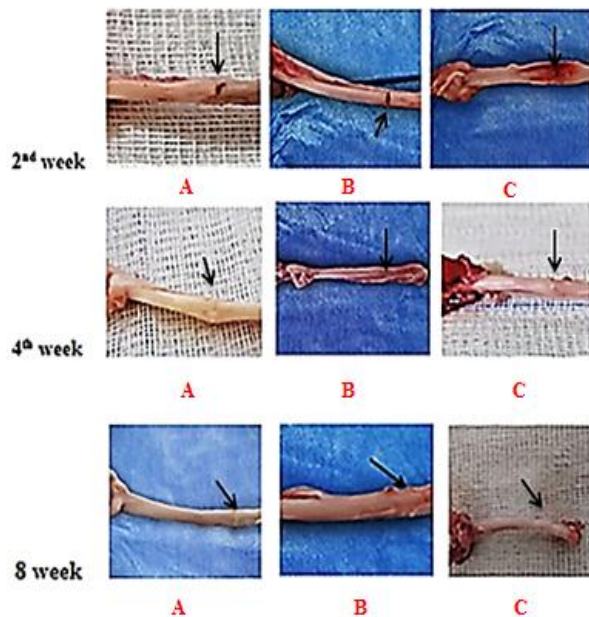
**Laboratory Evaluation of Magnesium Oxide Nanoparticle**

The Irritation test :Injected 1ml from each of carbopol, Alcohol, HA, MgONPs, HA+MgONPs, carbopol+ Alcohol +MgONPs, carbopol+ Al-cohol+ HA and carbopol+ Al-cohol+ HA+MgONPs. After 1h and B after 24h, observe the gel element's irritant before and after mixing with HA and MgONPs (Fig.5).



Figure, 5: Injected intradermal of : carbopol (a), Al-cohol+ NaOH (b), HA (c), MgONPs (d), HA+ MgONPs (e), carbopol+ Al-cohol+MgONPs (f), carbopol+ Al-cohol+ HA (g) and carbopol+ Al-cohol+ HA+ MgONPs (h). A after 1h. and B after 24h.

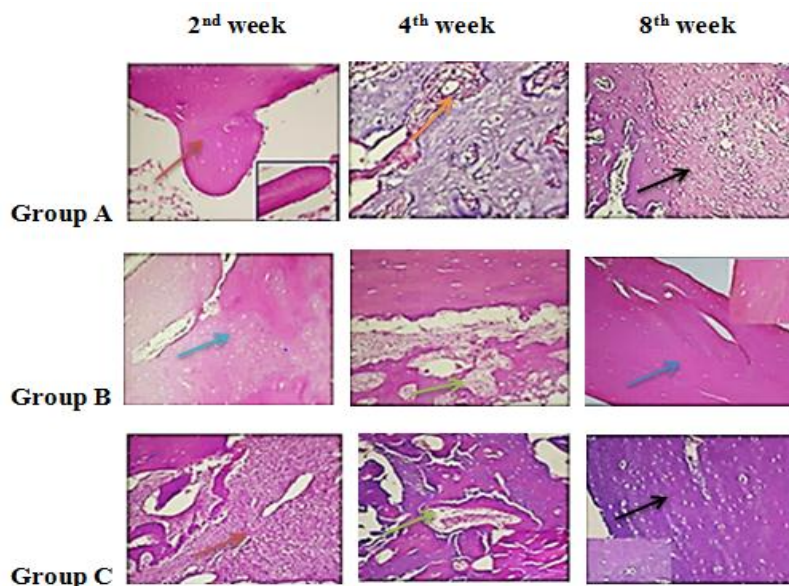
**Macroscopic Evaluation:** The macroscopical findings were determined while collecting the specimens for histopathological analysis after euthanizing the animals by using a high dose of ketamine hydrochloride and dissecting the radial bone from the surrounding tissue, and examined the degree of fracture healing grossly Fig. 6: In all groups at 2<sup>nd</sup>-week post-operation showed a bone reaction in a different degree which is more clear in groups B and C. In the 4<sup>th</sup> week in groups A, B and C partially connected, the fracture ended and displayed the fracture gap in groups B and C. At 8<sup>th</sup> week disappear the fracture line with remodelling it in groups A, B and C especially groups B and C that obtained like a normal bone shape Fig, 6



Figure, 6: macroscopic finding, at 2<sup>nd</sup> week post-operative showed little reaction in group A and B but more clearly in group C. At 4<sup>th</sup> week showed partial connected the fracture ends in group A and display the fracture line in group B and C. At 8<sup>th</sup> week showed display the fracture line in all groups but take the normal shape in groups B and C.

### Histopathological Evaluation

The histopathological sections in group A at 2<sup>nd</sup>-week post-operation showed trabecular bone lined by osteocyte with the moderate proliferation of mesenchymal tissue. At 4<sup>th</sup> week of the same group showed active osteoblast remnant of vascular congestion and at 8<sup>th</sup> week showed endochondral ossification with osteoid deposition and new hyaline cartilage formation. Group B at 2<sup>nd</sup> week showed hyaline cartilage with osteoblast lining. At 4<sup>th</sup> week lamellar bone with calcified osteoid tissues and hyaline cartilage. At 8<sup>th</sup> week post-operative revealed compact bone with fewer hyaline cartilage and several osteoids in lacuna with collagen. In group C at 2<sup>nd</sup>-week post-operative, evidence of endochondral ossification with the remnant of fibrous tissues. At 4<sup>th</sup> week compact bone with vascular bone developed and many osteocytes. At 8<sup>th</sup>-week postoperative compact bone formation Fig. 7.



Figure, 7: Histopathological findings in group A at 2<sup>nd</sup> week post-operative showed trabecular bone with osteoblast. At 4<sup>th</sup> weeks post-operation showed active osteoblast remnant of vascular congestion and at 8<sup>th</sup> weeks endochondral ossification with osteoid deposition. In group B at 2<sup>nd</sup> week post-operative showed hyaline cartilage and compact bone. At 4<sup>th</sup> week post-operative lamellar bone with calcified osteoid tissues. and at 8<sup>th</sup> week post-operative revealed compact bone with fewer hyaline cartilage. In group C at 2<sup>nd</sup> week post-operative evidence of endochondral ossification with remnant of fibrous tissues. At 4<sup>th</sup> week post-operative showed compact bone with vascular bone developed and many osteocyte. At 8<sup>th</sup> week compact bone formation.

## Discussion

### Laboratory Evaluation of Magnesium Oxide Nanoparticle

Atomic Force Microscopy (AFM): It can be seen the nanoparticles were spherical. The results showed a three dimensional (3D), and two dimensional (2D) images of synthesis MgONPs by *Alo vera* indicated uniformly arranged (24).

UV visible: UV-Vis spectroscopy shows a specific absorption peak at 267.6 nm, at the range of 200 to 300 nm, specific for MgONPs. This peak indicates a high purity of the synthesis MgONPs by *Alo vera*. It was observed that the bandgap of the sample constant, i.e. (7.5eV), for constant calcination temperature at 500 and 700°C (29).

### Laboratory Evaluation of Hydroxyapatite (HA)

XRF: The elemental analysis results agree with Koksal *et al.*, 2018. when showed in this method measured the following elements Ca, P, K, Cu, Fe, but in present HA artificial powder and normally found other elements as impurities arise from manufacturing process but with very little and unmentioned concentration. This ratio of Ca/ P of XRF results in the present study ensuring the HA had an excellent tensile strength, osteoconductivity and solubility, so XRF seemed to be a

good elemental analysis technique, especially it was a non-destructive technique (30).

Macroscopic Evaluation: Mixed MgONPs/ HA gave wonderful healing in the bone that differentiated in macroscopic and microscopic, that agree with (31) when confirmed biodegradation rate of hydroxyapatite doped with metal ions was slower than that pure mineral and when showed the rate of resorption appeared to be minimal when the material as mentioned above was a doped with Mg ion it occurs simultaneously with replacement by bony tissue and that agree with (32). HA/ Gel provided osteoconduction, and MgONPs provided enough vascularization. However, HA promoted fracture healing that agrees with (33) used Eggshell as a scaffold with stem cells. Bar MgO nanoparticles have a problem is limited by the low fracture toughness of MgO Incorporation into polymer composites that is a viable method for delivering MgO while fracture toughness increased for this reason used in this study MgONPs/HA/ gel and this agreement with (34)

Histopathological changes: group B and C gave better results, and that may be due to MgONPs are of enhancing bone regeneration for their benefits on bone cells forming and in at concentrations 200 µg/mL, MgONPs has been to improve and accelerate the proliferation of bone marrow-derived mesenchymal stem cells (BMSCs), that agree with (14, 34 and 35). HA is considered osteoinductive and osteoconductive, resulting in bone formation supported by some researchers (36 and 37). The hydrogel added to prolonged the period that had the potential to be a minimally invasive and robust cell delivery system that could allow for the sustained and controlled release of various drugs, growth factors and cells that agree with (38, 39 and 40). These unique properties allow for the application in the regeneration of bone, cartilage, neural tissue (40). Furthermore, situ gelation makes it an ideal filler for porous bone (41). Nano with HA/Gel is very good for remineralization of the enamel and cementum corresponding with our results, especially nanoparticle compatible with bone marrow structure and HA able o enhance the penetration and that agrees with (42) who used NHA/GEL on enamel and cementum. Studies of Hydrogel/HA/MgO nanocomposite can increase primary osteoblast density that agrees with (43). In the group B and C obtained more early and mature of osteoblast led to acceleration enhance of fracture and early compact bone formation with regular collagen, that conceded with (44) who explain the magnesium strongly involved in bone metabolism, as a mitogen factor for osteoblasts, and as a protective factor from excessive bone resorption.

## References

1. Marongiu G., Andrea Contini 1, Andrea Cozzi Lepri 2, Matthew Donadu 3 , Marco Verona 1 and Antonio Capone. The Treatment of Acute Diaphyseal Long-bones Fractures with Orthobiologics and Pharmacological Interventions for Bone Healing Enhancement: A Systematic Review of Clinical Evidence. Italy. MDPI, Bioengineering 2020, 7, 22; (1- 16). doi:10.3390/bioengineering7010022. www.mdpi.com/journal/bioengineering.
2. Saleh S.I and Omar R.A. Study of low power laser effect on the healing of tibial fracture treated by intramedullary pin in rabbits. University of Baghdad, Baghdad, Iraq. Iraqi Journal of Veterinary Sciences, 2003; 27(1):99- 107. <http://jcovm.uobaghdad.edu.iq>.

3. Ogoose A, Hotta T, Kawashima H, et al. Comparison of hydroxyapatite and beta tricalcium phosphate as bone substitutes after excision of bone tumors. *J. Biomed Mater. Res B Appl Biomater* 2005; 72: 94–101.
4. Shi H. , Ziqi Zhou 1,2, Wuda Li 1,2, Yuan Fan 1,2, Zhihua Li 1,2,\* and Junchao Wei. Hydroxyapatite Based Materials for Bone Tissue Engineering: A Brief and Comprehensive Introduction. China, MDPI, *Crystals* 2021, 11, 149. <https://doi.org/10.3390/cryst11020149>.
5. Fiume E., Giulia Magnaterra 1, Abbas Rahdar 2 , Enrica Verné 1 and Francesco Baino. Hydroxyapatite for Biomedical Applications: A Short Overview. MDPI, *Ceramics* 2021, 4, 542–563. <https://doi.org/10.3390/ceramics4040039>.
6. Grober, U., Schmidt, J., Kisters, K., Magnesium in Prevention and Therapy. *Nutrients*. (2015).7:(8199-8226).
7. Zhou H., Liang B. Jiang H., Deng Z., Yu K. Magnesium-based biomaterials as emerging agents for bone repair and regeneration: from mechanism to application. *Chongqing University China. J. of Mg Alloys*. 2021. 9: (779- 804). <https://doi.org/10.1016/j.jma.2021.03.004>.
8. Burmester A., Willumeit- Romer R., Feyerabend F. Behavior of bone cells in contact with magnesium implant material. *J. Biomed Mater. Res. B. Appl. Biomater.*(2017). 105:(165- 179).
9. Lin S., Yang G., Jiang F., Zhou M., Yin S., et al. A magnesium- enriched 3D culture system that mimics the bone development microenvironment for vascularized bone regeneration. (2019). *Adv. Sci*. 6: 1900209.
10. Farokhi M., Mottaghitab F., Reis R.L., Ramakrishna, S., Kundu S.C., Functionalized silk fibroin nanofibers as drug carriers: advantages and challenges. *J. Control. Release*. (2020). 321:(324- 347).
11. Sartori, M.; Giavaresi, G.; Tschon, M.; Martini, L.; Dolcini, L.; Fiorini, M.; Pressato, D.; Fini, M. Long-term in vivo experimental investigations on magnesium doped hydroxyapatite bone substitutes. *J. Mater. Sci. Mater. Med.* 2014, 25, 1495–1504. [CrossRef]
12. Lu, Y., Tao, P., Zhang, N., and Nie, S. (2020). Preparation and thermal stability evaluation of cellulose nanofibrils from bagasse pulp with differing hemicelluloses contents. *Carbohydr. Polym.* 245:116463. doi:10.1016/j.carbpol.2020.116463.
13. Wang, P., Yin, B., Dong, H., Zhang, Y., Zhang, Y., Chen, R., et al. (2020). Coupling biocompatible au nanoclusters and cellulose nanofibrils to prepare the antibacterial nanocomposite films. *Front. Bioeng. Biotechnol.* 8:986. doi: 10.3389/fbioe.2020.00986.
14. Zhang, Y., Wang, P., Mao, H., Zhang, Y., Zheng, L., Yu, P., et al. (2021). PEGylated gold nanoparticles promote osteogenic differentiation in in vitro and in vivo systems. *Mater. Des.* 197:109231. doi: 10.1016/j.matdes.2020.109231
15. Khandaker, M., Li, Y., and Morris, T. (2013). Micro and nano MgO particles for the improvement of fracture toughness of bone-cement interfaces. *J. Biomech.* 46,1035–1039. doi:10.1016/j.jbiomech.2012.12.006
16. Ke, D., Tarafder, S., Vahabzadeh, S., and Bose, S. (2019). Effects of MgO, ZnO, SrO, and SiO<sub>2</sub> in tricalcium phosphate scaffolds on in vitro gene expression and in vivo osteogenesis. *Mater. Sci. Eng. C Mater. Biol. Appl.* 96,10–19.
17. Roh, H.S., Lee C.M., Hwang Y.H., Kook M.S., Yang S.W., Lee D. Addition of MgO nanoparticles and plasma surface treatment of three-dimensional

- printed polycaprolactone/hydroxyapatite scaffolds for improving bone regeneration. *Mater Sci Eng C Mater Biol Appl*, 2017. 74: p. 525-535.
18. Sudakaran SV, Venugopal JR, Vijayakumar GP, et al. Sequel of MgO nanoparticles in PLACL nanofibers for anticancer therapy in synergy with curcumin/beta-cyclodextrin. *Mater Sci Eng C Mater Biol Appl* 2017, 71: 620–628.
  19. Syed-Picard FN, Shah GA, Costello BJ, et al. Regeneration of periosteum by human bone marrow stromal cell sheets. *J Oral Maxillofac Surg* 2014; 72: 1078–1083.
  20. Wang P, Zhao L, Liu J, et al. Bone tissue engineering via nanostructured calcium phosphate biomaterials and stem cells. *Bone Res* 2014; 2: 139–151
  21. Bigham-Sadegh A, IrajKarimi, MohamadShadkhast, Mohamad-HoseinMahdavi. (2015). Hydroxyapatite and demineralized calf fetal growth plate effects on bone healing in rabbit model. *J OrthopaedTraumatol* 16:141–149.
  22. Rasli N.I, Basri H\*, Harun Z.(2020). Zinc oxide from aloe vera extract: two-level factorial screening of biosynthesis parameters. *Batu Pahat, Johor, Malaysia. Heliyon* 6 e03156. Pp: 3-4.
  23. Diachenkoa O V, Opanasuyka A S, Kurbatova D I, Opanasuyka N M, Kononova O K, Namb D and Cheongb H (2016) Surface Morphology, Structural and Optical Properties of MgO Films Obtained by Spray Pyrolysis Technique. *Acta physica Polonica* 130(3), 805-810.
  24. Al-Salhi H.H and Al-Kalifawi E.J. (2020). Antibacterial and Antivirulence Activity of Magnesium Oxide Nanoparticles Synthesized Using *Klebsella Pneumonia* Culture Filtrate. University of Baghdad, Baghdad, Iraq. *Biochem. Cell. Arch.* 20(2): pp. 000-000.
  25. Beckhoff, B. B. Kanngiesser, N. Langhoff, R. Wedell, H. Wolf, Handbook of practical X-ray fluorescence analysis, Springer, Berlin, Germany (2006).
  26. Senyigit Z.A.; Karavana S.Y., Eraç B.; Gürsel O.; Limoncu M.H. and Baloğlu E. (2014) Evaluation of Chitosan-Based Vaginal Bioadhesive Gel Formulations for Antifungal Drugs *Acta Pharm.*; 64(2): 139-56. Doi: 10.2478/acph-2014-0013.
  27. Amin Bigham-Sadegh, IrajKarimi, MohamadShadkhast, Mohamad-HoseinMahdavi. (2015). Hydroxyapatite and demineralized calf fetal growth plate effects on bone healing in rabbit model. *J OrthopaedTraumatol* 16:141–149.
  28. Luna HT. (1968). Manual of histologic staining methods of the armed forces institute of pathology. 3rd
  29. Moorthy, S.K., Ashok, C.H., Rao, K.V., Viswanathan, C., 2015. Synthesis and characterization of MgO nanoparticles by neem leaves through green method. *Mater. Today: Proceedings* 2, 4360–4368. <https://10.1016/j.matpr.2015.10.027>.
  30. Koksall O K, Apaydin G, Cengiz E, Samel L, et al. (2018). Chemical analysis of artificial bone powders by energy dispersive X-ray fluorescence spectrometry (EDXRF). *Spectroscopy and spectro analysis. Turkey.* 38(8). Pp: 2645- 2649.
  31. Kalita SJ and Bhatt H.A (2007). nanocrystalline hydroxyapatite doped with magnesium and zinc: synthesis and characterization. *Mater Sci Eng.* 27 Pp: 837- 848 [CrossRef].
  32. Zakrzewski W, Dobrzynski M, Rybak Z, Szymonowicz M and Wiglusz R.J. (2020). Selected Nanomaterials' Application Enhanced with the Use of Stem

- Cell in Acceleration of Alveolar Bone Regeneration during Augmentation process. Poland. MDPI. 10(1216): 2-29.
33. Opris H, Dinu C, Baciut M. Baciut G, Mitre I, Crsan B, Armencea G, Prodan D.A, Bran S.(2020). The influence of Eggshell on bone regeneration in preclinical in vivo studies. Romania. *Biology*. MDPI. 9(476)Pp:2- 17.
  34. Wetteland C. L, Huinan Liu, et al.(2017). Magnesium Oxide Based Nanocomposites for Bone Repair. University of California, Riverside. Pp: 3- 7.
  35. Pourdanesh, F., et al., In vitro and in vivo evaluation of a new nanocomposite, containing high density polyethylene, tricalcium phosphate, hydroxyapatite, and magnesium oxide nanoparticles. *Mater Sci Eng C Mater Biol Appl*, 2014. 40: p. 382-8.
  36. Zakaria, S.M., et al., Nanophase hydroxyapatite as a biomaterial in advanced hard tissue engineering: a review. *Tissue Eng Part B Rev*, 2013. 19(5): p. 431-41.
  37. Cheng, L.; Ye, F.; Yang, R.; Lu, X.; Shi, Y.; Li, L. and Bu, H. (2010). Osteoinduction of hydroxyapatite/ $\beta$ -tricalcium phosphate bioceramics in mice with a fractured fibula. *Acta biomaterialia*, 6(4): 1569-1574.
  38. Lee, K.Y. and D.J. Mooney, Hydrogels for tissue engineering. *Chem Rev*, 2001. 101(7): p. 1869-79.
  39. Tan, H.P. and K.G. Marra, Injectable, Biodegradable Hydrogels for Tissue Engineering Applications. *Materials*, 2010. 3(3): p. 1746-1767.
  40. Munarin, F., et al., New perspectives in cell delivery systems for tissue regeneration: natural-derived injectable hydrogels. *J Appl Biomater Funct Mater*, 2012. 10(2): p. 67-81.
  41. Polo-Corrales, L., M. Latorre-Esteves, and J.E. Ramirez-Vick, Scaffold design for bone regeneration. *J Nanosci Nanotechnol*, 2014. 14(1): p. 15-56.
  42. Juntavee N, Juntavee A and Plonginras P (2018). Remineralization potential of nano- hydroxyapatite on enamel and cementum surrounding margin of computer- aided design and computer aided manufacturing ceramic restoration. Thailand. *Iner. J. Nanomed.* 13(2755-2765).
  43. Hickey D. J.; Ercan B.; Sun L.; Webster T. J. (2015). Adding MgO nanoparticle to hydroxyapatite -PLLA nanocomposites for improved bone tissue engineering application. *Acta biomaterailia*. Boston, USA. 14: 175-184.
  44. Janning C, Willbold E, Vogt C, Nellesen J, Meyer-Lindenberg A, Windhagen H, Thorey F, Witte F (2010) Magnesium hydroxide temporarily enhancing osteoblast activity and decreasing the osteoclast number in peri-implant bone remodelling. *Acta Biomater* 6(5):1861–1868.